

Margarita Y Simeonova<sup>1\*</sup>, Dragomir Krystev<sup>1</sup>, Galya Ivanova<sup>2</sup>, Isaac Abrahams<sup>3</sup>, Nely Georgieva<sup>4</sup> and Tsvetelina Angelova<sup>4</sup>

<sup>1</sup>Department of Polymer Engineering, University of Chemical Technology and Metallurgy, 8 Kl. Ohridski Blvd., 1756 Sofia, Bulgaria

<sup>2</sup>REQUIMTE-UCIBIO, Departamento de Química e Bioquímica, Faculdade de Ciências, Universidade do Porto, Rua do Campo Alegre, 4169-007 Porto, Portugal

<sup>3</sup>School of Biological and Chemical Sciences, Queen Mary University of London, Mile End Road, London E1 4NS, United Kingdom

<sup>4</sup>Department of Biotechnology, University of Chemical Technology and Metallurgy, 8 Kl. Ohridski Blvd., 1756 Sofia, Bulgaria

**Dates:** Received: 10 March, 2017; Accepted: 03 April, 2017; Published: 04 April, 2017

\*Corresponding author: Margarita Y Simeonova, Department of Polymer Engineering, University of Chemical Technology and Metallurgy, 8 Kliment Ohridski Blvd., 1756 Sofia, Bulgaria, Tel: (+359 2) 81 63 226; E-mail: msimeonova@uctm.edu

**Keywords:** Nanoparticles; Poly (butyl cyanoacrylate); Fluoroquinolones; Ciprofloxacin; In vitro antibacterial activity

<https://www.peertechz.com>

## Research Article

# Synthesis, Characterization and Antibacterial Activity of Ciprofloxacin Loaded Polymer Nanoparticles for Parenteral Application

## Abstract

Different polymerization techniques as particle formation processes for ciprofloxacin-loaded poly (butyl cyanoacrylate) nanoparticles (CfH-PBCN) were evaluated to choose the most appropriate in terms of the resulting nanoparticles characteristics suitable for parenteral administration. The formulations prepared by the selected technique were considered concerning size, size distribution, surface charge, loading efficiency, drug release. The mechanism of drug immobilization was also studied. Emulsion polymerization using 0.1 M HCl as an acidifying medium and Pluronic F68 as an emulsifier was found to be the best technique, leading to nanoparticles with a mean diameter below 300 nm, narrow size distribution, and a high drug payload of between 61-81 %. Analytical techniques (FTIR, GPC, XRD and <sup>1</sup>H NMR) are consistent with a strong covalent interaction between the drug and the polymer matrix of the nanoparticles. It is proposed that CfH is involved in the initiation of the polymerization process resulting in a modification of CfH molecule that could reduce its susceptibility to efflux in Gram-positive bacteria and eukaryotic cells. The antimicrobial activity of CfH-PBCN against *Bacillus subtilis* 3562 and *Escherichia coli* K12 is similar to that of the free drug and confirms that this activity is largely unaffected by the drug's association with the polymer nanoparticles.

## Introduction

Ciprofloxacin (1-cyclopropyl-6-fluoro-4-oxo-7-piperazin-1-yl-quinoline-3-carboxylic acid, Figure 1 is a second generation fluoroquinolone antibiotic, with a broad spectrum of activity against wild-type Gram-positive and Gram-negative organisms. Ciprofloxacin (CfH) is among the most effective antibiotics used clinically [1], and has become the drug of choice for a variety of topical applications [2]. However, due to its relatively short intracellular residence time, CfH is considered less effective than other fluoroquinolones, such as pefloxacin and ofloxacin, in some intracellular infections [3]. The recognition of CfH by the efflux transporters needs modulation in order to optimize its pharmacological profile. To overcome these disadvantages two different approaches have been proposed:

- i. Chemical modification of the CfH molecule [4,5].
- ii. Targeting the intracellular compartment using suitable drug delivery systems (DDS) able to prolong the intracellular residence time inside infected cells and to enhance the drug bioavailability.

A variety of DDS [6-13] has been studied in order to improve the specificity of the drug, to reach the sites where pathogens are harboured and to enhance the drug efficiency, including reducing bacterial biofilm formation [14]. The effectiveness of different poly (alkyl cyanoacrylate) (PACA) nanoparticles [15-17], as drug carriers for CfH, was investigated in an attempt to enhance its bioavailability in infected cells and hence improve its therapeutic efficiency. Although promising results were

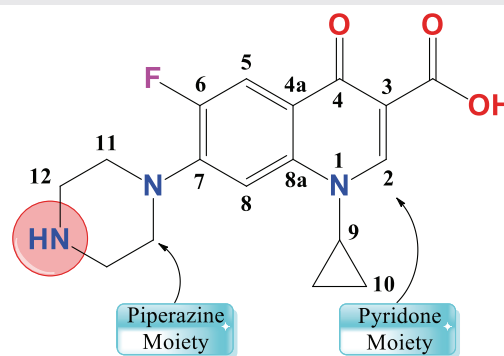


Figure 1: Molecular structure of Ciprofloxacin.

obtained for antibacterial activity in vitro, the inclusion of CfH into PACA nanoparticles resulted in incomplete eradication of Salmonella persisting in organs of the mononuclear phagocyte system [18], most probably due to some non-dividing intracellular bacteria with less susceptibility to antibiotic treatment [19].

In the present work, different polymerization techniques for the preparation of ciprofloxacin loaded poly (butyl cyanoacrylate) nanoparticles (CfH-PBCN) were analyzed to identify the most suitable in terms of the physicochemical properties of the resulting nanoparticles appropriate for parenteral administration. The formulations prepared by the selected polymerization technique were studied with respect to particle size and distribution, loading efficiency, and drug release. The mechanism of drug-polymer interaction was established, and the antibacterial activity of the chosen formulation was evaluated in vitro.

## Materials and Methods

### Materials

Ciprofloxacin, Pluronic F68, and citric acid as monohydrate were purchased from Sigma-Aldrich. Normal butyl-2-cyanoacrylate (n-BCA) was obtained from Specialty Polymers Ltd., Bulgaria, Dextran 40 (mol. wt. 40 000 g/mol) from Pharmachim, Bulgaria and DMSO- $d_6$  from CortecNet (France). Other chemicals were of laboratory grade purity and used as obtained.

### Preparation of ciprofloxacin-loaded nanoparticles

The CfH-PBCN were prepared by several techniques:

**Dispersion polymerization:** Dispersion polymerization was carried out in an acidified (citric acid, 0.2% w/v) aqueous medium, containing dextran 40 (0.8 % w/v) as a colloid stabilizer and ciprofloxacin (0.1- 0.4 mg/ml). The monomer was added carefully to the above aqueous medium under magnetic agitation. Polymerization was accomplished with or without addition of 4% v/v acetone in the polymerization medium. Polymerization started instantly and proceeded for ca. 3.5 h at room temperature. After the polymerization process ended, the pH of the resulting colloidal suspension was adjusted to a value of 5.5 using 1 N NaOH.

**Interfacial polymerization:** Polymerization was carried out in aqueous medium, acidified by citric acid (0.2% w/v), containing ciprofloxacin (0.1, 0.2 and 0.4 mg/ml) and Pluronic F68 (0.1 % w/v) as emulsifier. The monomer was dissolved in 1 ml acetone (organic phase) and added carefully to the aqueous mixture. Polymerization started instantly and was left to proceed as in 2.2.1.

**Emulsion Polymerization:** Polymerization was carried out in an aqueous medium, acidified (pH 2.5) either by citric acid (0.2% w/v) or 0.1 M HCl, containing ciprofloxacin (0.2-1.0 mg/ml) and Pluronic F68 (0.1 % w/v) as emulsifier. 200  $\mu$ l (4% v/v) of acetone were added to the polymerization medium immediately before monomer addition. Polymerization started

instantly after addition of the monomer and was left to proceed as in 2.2.1.

### Physicochemical characterization

**Dynamic light scattering and electrophoretic mobility measurements:** A Zetasizer Nano ZS (Malvern Instruments Ltd., UK) was used for particle size, size distribution and zeta potential measurements by dynamic light scattering and laser Doppler electrophoresis, respectively. Before analyses, the samples were appropriately diluted with deionized water. Size measurements were accomplished at a light scattering angle of 173° at 25 °C in a 12 mm square polystyrene cuvette (Sarstedt, Germany). The zeta potential measurements were performed at a light scattering angle of 17° at 25 °C, using a disposable capillary cell (DTS 1060, Malvern).

**Scanning electron microscopy analysis:** The morphology of unloaded and CfH-loaded nanoparticles was examined using a Philips SEM 515 (The Netherlands) scanning electron microscope, operated at 25 kV accelerating voltage. Samples were deposited on cover glasses, dried and then coated with a gold-palladium thin film using a 3C7620 Sputter Coater (Quorum Technologies Ltd., UK).

**Fourier transforms infrared (FTIR) spectroscopy characterization:** Unloaded and CfH-loaded nanoparticles, free CfH, and a physical mixture of unloaded nanoparticles and CfH were analyzed by FTIR spectroscopy. Spectra were recorded on KBr discs using a Varian Resolutions Pro spectrometer with a resolution of 2  $\text{cm}^{-1}$  in the 4000–400  $\text{cm}^{-1}$  spectral region.

**Gel Permeation Chromatography:** Molecular weight and molecular weight distributions of loaded and unloaded nanoparticles were determined by gel permeation chromatography (GPC). A Waters chromatographic system equipped with a differential refractometer M410, with a set of Phenogel 100 Å and Phenogel 10000 Å columns (Phenomenex), used simultaneously and calibrated with polystyrene standards was used. Tetrahydrofuran (THF) was used as a mobile phase, with a flow rate of 1.0 ml/min at 40 °C. Samples were dissolved in THF at a concentration of 4 mg/ml, and portions of 100  $\mu$ l of the solutions were injected into the chromatographic system. Data collection and processing were carried out using the Clarity software (DataApex)

**UV-visible spectroscopy characterization:** UV-Vis Spectroscopic measurements were performed on free and nanoparticle associated CfH in deionized water (pH 5) on a UV-1600 PC Spectrophotometer (VWR International Europe, Belgium), equipped with 10-mm quartz cells.

**Entrapment efficiency:** Samples of CfH-loaded nanoparticles were centrifuged at 15000 rpm for 1 h at 4 °C in a MIKRO 220R centrifuge (Hettich ZENTRIFUGEN, Germany). The supernatants were analyzed by UV-visible spectroscopy, and the concentration of free drug in the supernatant was determined by direct spectrophotometric analysis. Entrapment efficiency (EE) was calculated using the equation:  $EE (\%) = (\text{initial drug concentration} - \text{concentration in supernatant}) / \text{initial drug concentration} \times 100$ .

## In vitro drug release study

One ml of intact CfH-loaded PBCN (CfH 0.4 mg/ml) was introduced into a dialysis tube (MWCO 3 500 g/mol) and sealed. This dialysis tube was put into a 50 ml Erlenmeyer flask with 25 ml of phosphate buffered saline (PBS, pH 5.5). Release tests were performed at  $37 \pm 0.5$  °C under mild stirring. At predetermined times, 1 ml aliquots of the release medium were taken and subsequently replaced with fresh medium. Each aliquot was assayed for CfH using UV-visible spectroscopy at 277 nm.

## NMR analysis

$^1\text{H}$  NMR spectra, recorded on a Bruker Avance III 400 spectrometer at a temperature of 25 °C in dimethyl sulfoxide- $d_6$  (DMSO- $d_6$ ) solution were referenced to the solvent resonance peak at 2.49 ppm. Proton registered diffusion-ordered NMR ( $^1\text{H}$  DOSY) experiments were acquired using a 2D sequence for diffusion measurements, with stimulated echo and bipolar gradient pulses (stebpgp1s, Bruker library) as the experimental conditions (amount of the solute and the solvent, temperature, air flow, no sample rotation) were kept constant. In each experiment, 32 spectra of 32 k data points were collected, with values for the duration of the magnetic field pulse gradients ( $\delta$ ) of 4 and 2.8 ms, diffusion times ( $\Delta$ ) of 200 and 150 ms for nanoparticles (unloaded and drug-loaded) and free CfH, respectively. The pulse gradient ( $g$ ) was incremented from 2 to 95% of the maximum gradient strength in a linear ramp. All spectra were processed using the Bruker Topspin software package (version 3.2). The diffusion coefficients ( $D$ ) were obtained by measuring the signal intensity at more than one place in the spectra. At least two different measurements were performed for the determination of each diffusion coefficient. The water in the solvent (DMSO- $d_6$ ) (resonance at 3.3 ppm,  $D_{\text{water}} = 1.56 \times 10^{-9} \text{ m}^2\text{s}^{-1}$ , calculated standard deviation of  $1.9 \times 10^{-3}$ ) was used as an internal reference for the diffusion measurements.

## X-ray powder diffraction

X-ray powder diffraction data were collected on a PANalytical X'Pert Pro diffractometer using Ni filtered Cu  $K\alpha$  ( $\lambda = 1.5418 \text{ \AA}$ ) in flat plate  $\theta/\theta$  geometry. Data were acquired over the  $2\theta$  range 3 to 70°, in steps of 0.0334°, with an effective counting time of 200 s per step. Data were calibrated with an external  $\text{LaB}_6$  standard.

## Antibacterial activity

The antibacterial activity of free CfH, unloaded and CfH loaded nanoparticles was tested *in vitro* against Gram-positive *Bacillus subtilis* 3562 and facultative anaerobic Gram-negative *Escherichia coli* K12, using the agar disk diffusion method, and an assay based on the reduction of viable bacterial cells after exposure to the tested compounds. The strains obtained from the culture collection of the Bulgarian National Bank of Industrial Microorganisms and Cell Cultures were cultured in Luria-Bertani (LB) medium.

**Agar disk diffusion method:** The overnight bacteria cultures from tested strains were prepared in a liquid LB medium. A

single colony was used for inoculating the liquid LB medium to maintain an initial bacterial concentration of  $1 \times 10^6$  cfu/ml for *B. subtilis* 3562, and  $1 \times 10^7$  cfu/ml for *E. coli* K12. Bacterial suspensions (100  $\mu\text{l}$ ) were seeded on agar plates with solid LB medium. After 30 min, sterile paper disks (6 mm in diameter) were soaked with 6  $\mu\text{l}$  of the test compound, and placed on the surface of the agar plate. The plates were incubated for 24 hours at 30 °C for *B. subtilis* 3562 and at 37 °C for *E. coli* K12. The sizes of resulting inhibition zones were measured. The untreated bacterial cultures were used as blank, while those treated with polymerization medium served as negative controls. Mean values of the inhibition zones were determined by performing the experiments in triplicate.

**Antimicrobial activity based on the number of surviving cells on agar plates:** Microbial growth-inhibiting effects of the tested compounds were further evaluated by studying the ability of the used strains to survive after drug exposure. For this purpose, 100  $\mu\text{l}$  of strain suspension and 50  $\mu\text{l}$  of each compound were added to flasks containing 50 ml saline solution. The incubation was done on a rotary shaker (220 rpm) for different time intervals at 30 °C or 37°C for *B. subtilis* 3562 and *E. coli* K12, respectively. Aliquots (100  $\mu\text{l}$ ) were taken after 5, 24 and 48 hours, and dropped on the agar surface. Further, the plates were incubated for 24 hours at a temperature, appropriate for the strains. The number of colony-forming units (CFU) from the plates was subsequently counted. To evaluate the antibacterial effect of the tested compounds, the percentage of cell reduction was calculated using the equation: Cell reduction (%) =  $(1 - \text{Test sample (CFU/ml)}/\text{Control (CFU/ml)}) \times 100$  [20]. Samples of untreated bacterial cells were used as controls. The measurements were made in duplicate.

## Results and Discussion

The most frequently used method for preparation of PACA nanoparticles is based on the *in situ* polymerization of monomers in different aqueous media. Depending on the presence of either emulsifier or colloid stabilizer, two types of polymerization techniques, emulsion and dispersion polymerization, respectively are adopted. Alkyl-2-cyanoacrylate monomers are also capable of undergoing interfacial polymerization, where polymerization occurs at the interface between the dispersed (organic) and the continuous (aqueous) phase, leading to the formation of nanoparticles.

The anionic mechanism of polymerization typically involves hydroxyl ions from the aqueous medium as initiators. However, during the polymerization process, activated monomer molecules can interact with drug molecules, dissolved in the polymerization medium, that possess basic functional groups, which can act as initiators.

Different polymerization techniques for the preparation of CfH loaded PBCN nanoparticles were evaluated and are discussed below.

CfH-PBCN prepared by dispersion polymerization showed a bimodal size distribution (Figure 2), with a high polydispersity index, PDI (0.122 – 0.501) (Table 1). The increase of the

drug equilibrium concentration leads to an increase in PDI. The extremely high dispersity of CfH-PBCN formulations make them inappropriate for medical applications, as better targeting can be achieved by monodisperse systems, since only particles of specific sizes are accumulated in the target tissues. No clear dependence of drug entrapment and polydispersity on the presence or absence of acetone in the polymerization system was observed, although it is known that acetone is able to diminish the aggregation of the obtained polymer chains by increasing the monomer diffusion from monomer droplet to aqueous phase [17]. Further, experiments using the dispersion polymerization method were therefore discontinued.

Nanoparticles prepared by interfacial polymerization have a satisfactory mean diameter, but the maximum drug loading of 0.010 mg/mg is reached at around 0.3 mg/ml concentration of CfH in the medium (Table 2). Furthermore, the PDI increases above this equilibrium drug concentration. These unfavorable findings indicate that interfacial polymerization is unsuitable for the preparation of CfH-PBCN for parenteral administration.

The mean diameters of the synthesized unloaded and ciprofloxacin-loaded nanoparticles prepared using emulsion

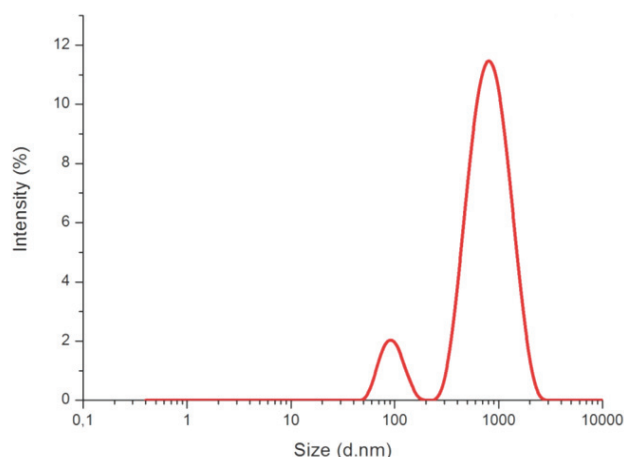


**Figure 2:** Typical size distribution by intensity of CfH-PBCN, prepared by dispersion polymerization.

**Table 1:** Physicochemical characteristics of CfH-PBCN, prepared by dispersion anionic polymerization (citric acid 0.2 % w/v, dextran 40, 0.8 % w/v, with or without 4% v/v acetone).

Concentration of CfH (mg/ml)	z-average diameter, (nm)	PDI	$\zeta$ -potential $\pm$ SD (mV)	Entrapment efficiency %	Loading capacity
0	152.8	0.008	-9.30 $\pm$ 5.10	-	-
0.2 <sup>a</sup>	195.0	0.157	-9.41 $\pm$ 4.03	58.13	0.006
0.2 <sup>b</sup>	187.0	0.122	-11.30 $\pm$ 4.83	59.90	0.006
0.3 <sup>a</sup>	179.8	0.366	-10.40 $\pm$ 5.56	68.74	0.010
0.3 <sup>b</sup>	215.3	0.370	11.20 $\pm$ 4.63	56.63	0.008
0.4 <sup>a</sup>	187.1	0.383	-10.00 $\pm$ 4.50	N	
0.4 <sup>b</sup>	254.6	0.501	-8.36 $\pm$ 4.10	N	

a-without acetone; b-with acetone;  
N-not measured

**Table 2:** Physicochemical characteristics of CfH-PBCN, prepared by interfacial polymerization (citric acid 0.2 % w/v and Pluronic F68 0.1 % w/v).

Concentration of ciprofloxacin (mg/ml)	z-average diameter, $d_z$ (nm)	PDI	$\zeta$ -potential $\pm$ SD (mV)	Entrapment efficiency %	Loading capacity (mg/mg)
0	182.3	0.076	-13.90 $\pm$ 5.61	-	-
0.2	229.3	0.078	-20.40 $\pm$ 10.30	65.32	0.007
0.3	247.2	0.088	-24.10 $\pm$ 9.57	69.97	0.010
0.4	229.4	0.136	-20.90 $\pm$ 8.16	51.05	0.010

polymerization were found to be greater than 311 nm, when citric acid was used as an acidifying agent (Table 3). The size distribution was wide, with PDI values between 0.143–0.177. The surfaces of both loaded and unloaded nanoparticles were negatively charged. The measured values of z-potentials for CfH-PBCN (-26.4 – -27.5 mV) were lower than that of unloaded nanoparticles (-22.7 mV). Therefore, the emulsion polymerization technique using citric acid as an acidifying agent was considered inappropriate for the preparation of CfH-PBCN, despite the high drug entrapment efficiency.

The physicochemical characteristics of ciprofloxacin-loaded nanoparticles formulations prepared by emulsion polymerization using 0.1 M HCl are presented in table 4. It can be seen that on drug inclusion, there is a general decrease in z-average diameters of the nanoparticles, probably as a result of the nanoparticles becoming more compact. The nanoparticles show a narrow size distribution with PDI values ranging from 0.003 to 0.071. The surfaces of both CfH-loaded and unloaded PBCN are negatively charged. However, the z-potentials for all CfH-PBCN are higher than that of PBCN, but show no direct correlation with the equilibrium drug concentration used.

Entrapment efficacy increases with increasing equilibrium drug concentration up to around 0.9 mg/ml ciprofloxacin (Table 4). This is reflected in an increase in drug loading capacity, with the maximum value of 0.041 mg/mg attained at 1.0 mg/ml ciprofloxacin.

The data obtained by different polymerization techniques of nBCA evidence the strong dependence of main nanoparticles characteristics on the method of nanoparticles preparation. Uniformity of nanoparticles (z-average diameter and polydispersity), surface charge and drug loading appear a function of the emulsifier/colloid stabilizer and acidifying agent used.

Due to the favorable properties of nanoparticles prepared by emulsion polymerization (Pluronic F68 0.1%, 0.1M HCl as an acidifying agent and 4% acetone), further analysis was restricted to these samples.

SEM micrographs of unloaded and ciprofloxacin-loaded PBCN (Figure 3) display a spherical shape and mean diameters consistent with those measured by DLS. The presence of CfH in the polymer matrix of the nanoparticles was confirmed by comparison of unloaded and drug-loaded nanoparticles

under UV illumination (figure insertions). Visual inspection of photographs clearly shows the presence of drug in the dry CfH loaded formulation (Figure 3b).

Unloaded and ciprofloxacin-loaded nanoparticles show a narrow molecular weight distribution (GPC profiles are not shown) with dispersity D (Mw/Mn) values of 1.03 and 1.07, respectively. The weight average molecular weight (Mw) of unloaded PBCN of 981 Da is consistent with the presence of oligomeric chains ( $n \approx 7$ ) and is typical for anionic polymerization of alkyl-2-cyanoacrylates in water [21].

The presence of CfH in the polymerization medium resulted in a change in the GPC profile, with the appearance of a small fraction of about 4% with Mw of 23608 Da and a main fraction with Mw of 10302 Da. This order of magnitude increase in Mw of ciprofloxacin-loaded nanoparticles as compared to unloaded nanoparticles suggests a chemical interaction of CfH with n-BCA during the polymerization process. This most probably occurs through the CfH molecule acting as an initiator in the polymerization process. The nitrogen atom of the imino group (NH) in the piperazine moiety of the CfH molecule (Figure 1) is electron rich and could act as a nucleophilic center able to attack the carbon-carbon double bond of n-BCA, resulting in the drug molecule addition and formation of a zwitterionic species (Scheme 1). The latter is able to initiate the polymerization via a zwitterionic mechanism while the elongation of the polymer chains occurs according to an anionic polymerization mechanism.

**Table 3:** Physicochemical characteristics of CfH-PBCN, prepared by emulsion polymerization (using Pluronic F68 0.1% w/v, citric acid 0.2% w/v and 4% v/v acetone).

Concentration of ciprofloxacin (mg/ml)	z-average diameter, $d_z$ (nm)	PDI	$\zeta$ - potential $\pm$ SD (mV)	EE %	Loading capacity (mg/mg)
0	329.4	0.163	-22.70 $\pm$ 6.24	-	-
0.2	311.9	0.156	-27.00 $\pm$ 8.62	72.15	0.007
0.4	575.5	0.143	-27.50 $\pm$ 8.65	70.01	0.014
0.6	411.0	0.177	-26.40 $\pm$ 7.71	N	N

**Table 4:** Physicochemical characteristics of CfH-PBCN, prepared by emulsion polymerization (using Pluronic F68 0.1%, 0.1M HCl as an acidifying agent and 4% v/v acetone).

Concentration of ciprofloxacin (mg/ml)	z-average diameter, $d_z$ (nm)	PDI	$\zeta$ - potential $\pm$ SD (mV)	EE (%)	Loading capacity (mg/mg)
0	260.6	0.049	-22.20 $\pm$ 11.40	-	-
0.2	255.0	0.099	-15.9 $\pm$ 5.27/	61.7	0.006
0.3	238.1	0.031	-20.10 $\pm$ 10.30	71.52	0.011
0.4	242.6	0.003	-20.60 $\pm$ 9.93	73.53	0.015
0.5	236.8	0.047	-19.30 $\pm$ 10.40	75.78	0.019
0.6	233.3	0.069	-18.50 $\pm$ 11.20	76.27	0.023
0.7	236.6	0.061	-16.60 $\pm$ 9.85	77.15	0.027
0.8	226.8	0.071	-15.80 $\pm$ 9.37	75.06	0.032
0.9	264.9	0.030	-18.80 $\pm$ 9.90	81.96	0.037
1.0	229.9	0.037	-20.70 $\pm$ 10.10	81.41	0.041

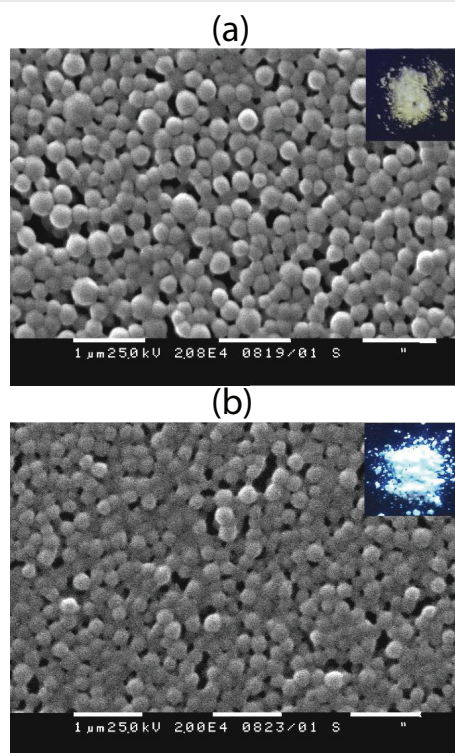
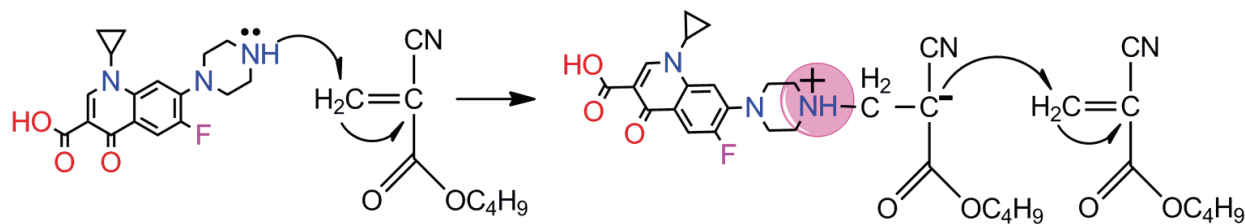


**Figure 3:** SEM micrographs of (a) unloaded and (b) CfH loaded PBCN (CfH 0.4 mg/ml); figure insertions represent photographs of dry samples of unloaded and ciprofloxacin-loaded PBCN, respectively under UV illumination.

The observed increase in the Mw of CfH-loaded nanoparticles could be a result of the coupling reaction between different ends of two or more zwitterionic chain ends and is in accordance with such an initiation mechanism, leading to an effective doubling of the polymer chain length. Although an acid, the CfH molecule shows amphoteric behavior in aqueous solutions due to the acid-base interaction between the piperazine basic nitrogen and the carboxylic group [22]. This acid-base interaction gives a weak basic character to the drug and the possibility of initiating the polymerization of cyanoacrylates via zwitterion formation. Analogous zwitterionic initiation of n-BCA polymerization by imino moieties in 5-fluorouracil molecules has been reported previously [23,15] assumed interaction between CfH and isobutylcyanoacrylate during the polymerization process when preparing CfH-loaded poly (isobutyl cyanoacrylate) nanoparticles, leading to initiation of polymerization through a zwitterionic pathway. The involvement of CfH in the polymerization of 2-ethylbutyl cyanoacrylate during the formation of poly (ethylbutyl cyanoacrylate) nanoparticles was described by Page-Clisson et al. [17]. However, these authors proposed an anionic mechanism of initiation of the polymerization of 2-ethylbutyl cyanoacrylate based on the significantly smaller Mw found for CfH-loaded nanoparticles.

It is important to note that Beyer et al. [24] suggested that the introduction of hydrophobic substituents in position C-7 (piperazine ring) of fluoroquinolones may reduce their susceptibility to efflux in Gram-positive organisms. Recently, Marquez et al. [5] demonstrated that addition of a bulky, lipophilic side chain on the CfH molecule at the same



**Scheme 1:** Zwitterionic mechanism of initiation of polymerization of n-butyl cyanoacrylate via nitrogen atom of the imino group (NH) in the piperazine moiety of the CfH molecule.

position (N-substituted) resulted in a markedly modified pharmacological profile of the drug, due to its reduced susceptibility to efflux in Gram-positive bacteria and eukaryotic cells and an increased accumulation in eukaryotic cells, without affecting either subcellular distribution or intracellular activity. Other authors have also considered the structural differences in fluoroquinolones, especially overall molecular hydrophobicity and bulkiness of the C-7 substituent as factors influencing the efficiency of efflux [25-29].

It can be argued that the covalent bond between the NH of CfH and the hydrophobic poly (butyl cyanoacrylate) chain, formed during the initiation process in the present study is a similar modification of the CfH molecule and could act in a similar way in reducing susceptibility to efflux in Gram-positive bacteria and eukaryotic cells.

The UV-visible spectra of free CfH and CfH-PBCN are shown in figure 4a. The inclusion of the CfH into the nanoparticles substantially changes its absorption spectrum. Three distinct absorption bands at 216, 277 and 315 nm are seen for free CfH. The latter two bands are greatly reduced in intensity in CfH-PBCN and are consistent with a chemical interaction between the drug molecule and the polymer matrix.

The FT-IR spectra of unloaded and ciprofloxacin-loaded PBCN are compared with that of the free drug and a physical mixture of the CfH and unloaded nanoparticles in figure 4b. In the spectrum of the free drug, the absorption bands at 1616.17  $\text{cm}^{-1}$  and 1724  $\text{cm}^{-1}$  are attributed to the symmetric stretching of C=O of pyridone and carboxylic moieties, respectively [30], while that at 1588.42  $\text{cm}^{-1}$  is due to the C=C stretching mode. The stretching vibration at 3403  $\text{cm}^{-1}$  is assigned to the OH in the carboxylic group. C-N stretching is seen at 1284.88  $\text{cm}^{-1}$ . The absorption band at 1035  $\text{cm}^{-1}$  is assigned to the C-F stretching vibration, while the vibration at 721  $\text{cm}^{-1}$  indicates the absorption peak of secondary amine (-NH).

The FT-IR spectrum of the unloaded nanoparticles shows characteristic bands for the poly(butyl cyanoacrylate): the  $\text{CH}_3$  asymmetric and symmetric vibration at 2959  $\text{cm}^{-1}$  and 2878  $\text{cm}^{-1}$ , respectively and asymmetric  $\text{CH}_2$  at 2934  $\text{cm}^{-1}$ , CN stretching at 2246  $\text{cm}^{-1}$ , C=O stretching at 1751  $\text{cm}^{-1}$ , asymmetric and symmetric C-O-C stretches at 1257 and 1018  $\text{cm}^{-1}$ , respectively, C-CN band at 1169  $\text{cm}^{-1}$  and OH at 3479.31  $\text{cm}^{-1}$  included in the polymer chain from water during initiation of polymerization.

The FT-IR spectrum of the physical mixture of unloaded PBCN and free CfH shows the characteristic bands for both

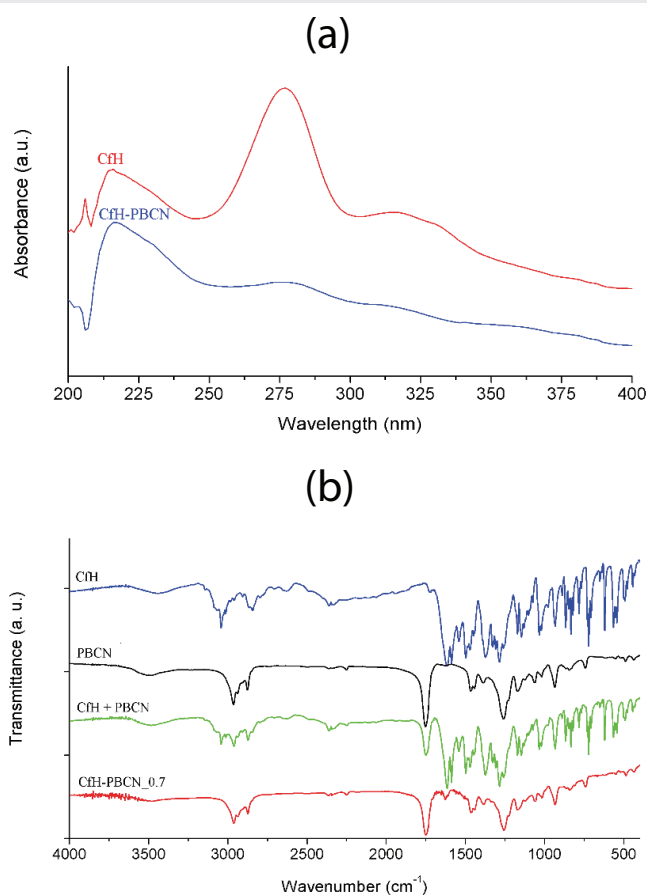


**Figure 4:** UV-visible spectra of CfH and CfH-PBCN taken in aqueous medium (a) and FT-IR spectra of free CfH, unloaded PBCN, a physical mixture of blank PBCN and CfH, and CfH-PBCN (CfH 0.7 mg/ml) (b).

compounds. In contrast, the characteristic bands of the CfH molecule are greatly reduced in intensity compared to the physical mixture in the FT-IR spectrum of CfH-PBCN. All bands characteristic for poly (butyl cyanoacrylate) are visible. The characteristic band assigned to quinolones at 1627.87  $\text{cm}^{-1}$  is clearly observed, confirming the presence of CfH molecules in the polymer matrix of nanoparticles. The disappearance of the absorption band at 721  $\text{cm}^{-1}$  suggests the possible involvement of the imino group in drug-polymer interaction.

$^1\text{H}$  NMR spectra of the studied samples are shown in figure 5a, along with the assignment of CfH and PBCN resonances. In the  $^1\text{H}$  NMR spectra of all CfH-PBCN samples, intense and broad resonance signals of poly(butylcyanoacrylate) protons

and very weak signals with variable intensity belonging to CfH protons, were clearly observed (Figure 5a,c-f). The ratios of n-BCA units to CfH, calculated from the integrated intensities of signals in the  $^1\text{H}$  NMR spectra of drug loaded PBCN, were found to be 33 : 0.77, 33 : 0.62, 33 : 0.42 and 33 : 0.22, for PBCN loaded with 1.0, 0.8, 0.6 and 0.4 mg/ml CfH, respectively. The signal for the piperazinyl imino proton was not observed in the spectra of the loaded nanoparticles, consistent with chemical interaction between the drug and the polymer chain via the imino group.

We further applied  $^1\text{H}$  DOSY to evaluate the mechanism of CfH immobilization into the polymer matrix of PBCN. The diffusion coefficients ( $D$ ) of CfH and poly (butylcyanoacrylate) in CfH-loaded PBCN were measured and compared with the corresponding values, obtained for free CfH and unloaded PBCN. The  $D$  values of CfH and PBCN were determined from the resonance signals of the aromatic protons of CfH and methyl protons of poly (butylcyanoacrylate) in the  $^1\text{H}$  NMR spectra. To account for changes in the samples viscosity the measured  $D$  values were all scaled to those of the internal standard ( $1.56 \times 10^{-9} \text{ m}^2\text{s}^{-1}$ ). The results are presented in figure 5b.

The measured diffusion coefficients for CfH in the drug loaded PBCNs were found to be significantly smaller than those of the free CfH and similar to the corresponding value of the unloaded PBCN. Increasing the amount of CfH in the drug loaded PBCN samples was found to slightly increase the diffusion coefficient of both the CfH and PBCN. The significant reduction of the  $D$  values of CfH in drug loaded PBCN is a strong indication of an association process between CfH and PBCN. The measured diffusion coefficients for the drug were considered as weighted-average values between the free CfH molecules and those bound to the polymer chains. The percentage of the bound CfH was determined using the equation [31,32] :  $D = f_{\text{free}} D_{\text{free}} + f_{\text{bound}} D_{\text{bound}}$

where  $D$  and  $f$  are the diffusion coefficients and molecular fractions of the free and bound CfH molecule and  $f_{\text{free}} + f_{\text{bound}} = 1$ . The fraction of CfH bound to the polymer chains of PBCN was found to be between 0.82 and 0.85. The disappearance of the piperazinyl imino proton of CfH in the drug loading process and the significant changes in the CfH diffusion coefficient to values similar to those of PBCN reveal a strong drug-polymer interaction and formation of a chemical bond.

Figure 6 shows the X-ray powder diffraction pattern for the CfH-PBCN sample with the highest loading compared to those of the unloaded nanoparticles and pure CfH. The patterns of both the drug loaded and unloaded nanoparticles show broad features characteristic of amorphous solids. There is little significant difference in their patterns, other than a small increase in intensity of the broad halo centered at around  $17.5^\circ$   $2\theta$  in the drug loaded sample. There is no evidence in the pattern for the CfH loaded nanoparticles for crystalline CfH, indicating the drug molecules do not order on the crystallographic scale. This is consistent with incorporation of drug molecules directly

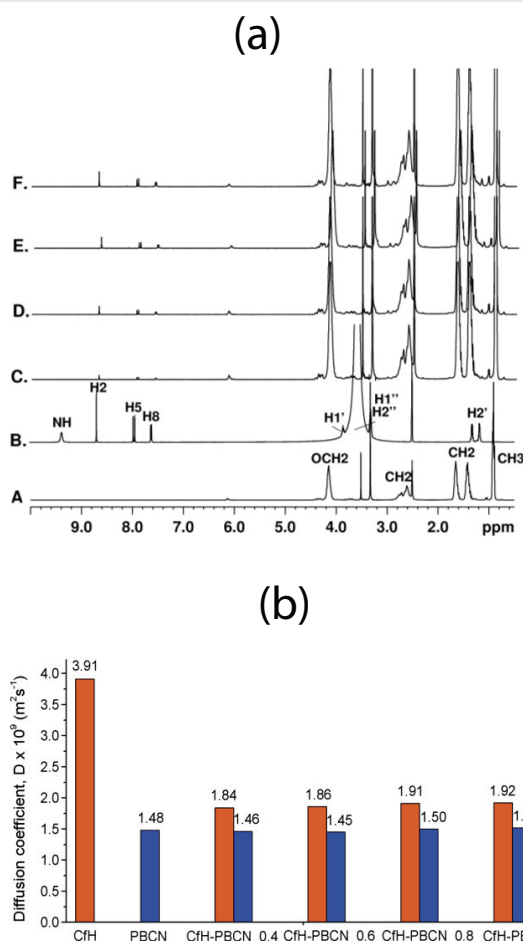


**Figure 5:**  $^1\text{H}$  NMR spectra (a) of: A. Blank PBCN; B. CfH; C-F. CfH (0.4 to 1.0 mg/ml) included in PBCN during the emulsion polymerization and diffusion coefficients (b) of free CfH, unloaded PBCN and PBCN with different CfH loadings (CfH-PBCN).

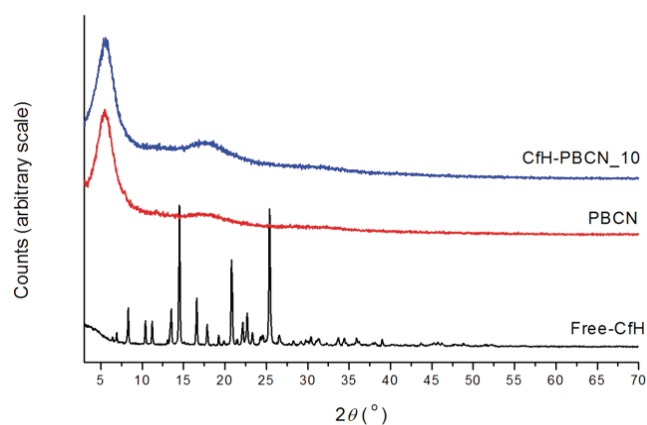


**Figure 6:** X-ray powder diffraction patterns for drug-loaded (CfH-PBCN\_1.0) and unloaded nanoparticles (PBCN) compared to that of pure CfH.

into the polymer matrix through chemical bonding rather than physical encapsulation.

*In vitro* drug release of CfH was studied in phosphate buffered saline (PBS) with pH 5.5 as above this pH value CfH became insoluble and precipitated. Indeed, as a consequence of the zwitterionic behavior of CfH its aqueous solubility at pH

values close to 7 (isoelectric point of the molecule) is low [33]. As figure 7 shows, the nanoparticles release only about 19.9% of their drug content. This drug release profile is indicative of a strong drug-polymer interaction.

A similar release profile of CfH associated to poly (ethylbutyl cyanoacrylate) nanoparticles was described by Page-Glisson et al. [17]. The authors reported no significant drug release in phosphate-buffered saline, or very slow drug release of 22.3% after 6 h of incubation in esterase enriched medium.

The antibacterial properties of ciprofloxacin-loaded and unloaded PBCN were tested *in vitro* against *Bacillus subtilis* 3562 and *Escherichia coli* K12 and compared with those of free CfH. Firstly, the agar disk diffusion method was used. Samples of the polymerization medium and the unloaded PBCN failed to form bacteria free zones (Figure 8). In contrast, free CfH formed a 7 mm inhibition zone for both strains, while CfH-PBCN formed 4 mm zones, confirming their antibacterial activity.

The second method revealed the number of viable cells of *B. subtilis* 3562 and *E. coli* K12 strains after different time exposure to the tested compounds. The pure strain cultures were defined as untreated controls. The results for *B. subtilis* 3562 and for *E. coli* K12 are presented in tables 5,6 respectively. Unloaded PBCN gave no reduction in the number of viable cells of both strains. Bacterial strains of *B. subtilis* 3562 and *E. coli* K12 exposed to free CfH exhibited a reduction of 99.3 % and 99.7 % of the viable cells after 48 h of exposure, respectively.

The exposure of both strains to CfH-PBCN led to comparable values of cells reduction, ascribed to the retained activity of CfH, which was not impaired by the inclusion process into the polymer matrix of nanoparticles. The decreasing of CFU caused by the free CfH and CfH-PBCN was observed even after 5 h of cells incubation, where the cell reduction was close to 90 % for *B. subtilis* 3562 (Table 5) and 81% for *E. coli* K12 (Table 6). After 48 h almost all of the bacteria lost their viability, showing that the time-dependent antimicrobial effect of CfH is largely unaffected by its association with PBCN.

The results from the microbial study confirm retained antibacterial activity after drug inclusion into the polymer matrix of nanoparticles. The findings prove that the fluoroquinolone key pharmacophore is unaffected by the immobilization process.

## Conclusion

This study analyzed the preparation techniques required to obtain spherical CfH-PBCN suitable for parenteral administration. On the basis of the nanoparticle characteristics, emulsion polymerization was chosen as the most acceptable technique for preparation of ciprofloxacin-loaded poly (butyl cyanoacrylate) nanoparticles. CfH is proposed as an initiator of the polymerization of n-BCA through the imino group in piperazine moiety. The results obtained strongly suggest covalent bonding between the CfH molecule and the polymer chains that could reduce its susceptibility to efflux in Gram-positive bacteria and eukaryotic cells. Thus we realize an

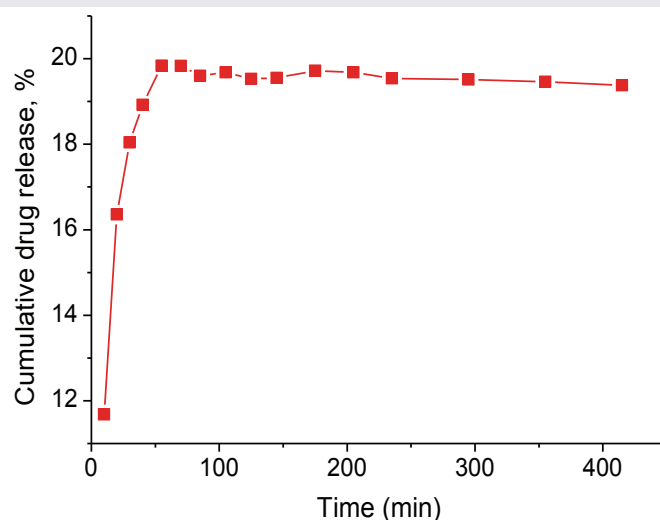


Figure 7: *In vitro* drug release profile of CfH from CfH-PBCN in PBS (pH 5.5) at 37 ± 0.5 °C.

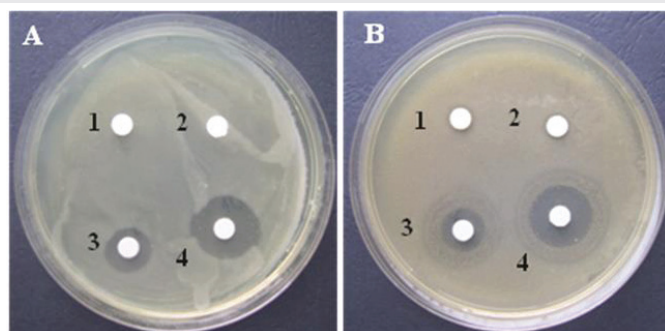


Figure 8: Antibacterial activity measured by the agar disk-diffusion method against *B. subtilis* 3562 (A) and *E. coli* K12 (B) as test microorganisms: 1-polymerization medium; 2- PBCN (2000 µg/ml); 3- CfH-PBCN (40-2000 µg/ml); 4- CfH (40 µg/ml).

Table 5: Antibacterial activity of unloaded and ciprofloxacin-loaded nanoparticles, compared to that of free CfH against *Bacillus subtilis* 3562.

Samples	Time of incubation [h]					
	5		24		48	
	CFU/ml × 10 <sup>-5</sup>	Reduction of cells [%]	CFU/ml × 10 <sup>-5</sup>	Reduction of cells [%]	CFU/ml × 10 <sup>-5</sup>	Reduction of cells [%]
<i>B. subtilis</i> 3562 (untreated control)	6.4	-	5.9	-	7.8	-
PBCN (control) 2000 µg/ml	6.4	-	5.9	-	7.8	-
CfH-PBCN (40/2000) µg/ml	0.63	90.1	0.58	98.9	0.15	98.0
CfH (40 µg/ml)	0.52	91.8	0.31	99.4	0.05	99.3

approach that combines the two proposed solutions for optimization of pharmacologic profile of CfH, a chemical modification of its molecule and targeting the intracellular compartment using suitable drug delivery systems. Antibacterial activity is largely unaffected by association of the CfH molecule with the polymer chains building the nanoparticles, showing similar time-dependent antimicrobial activity against both Gram-positive and Gram-negative bacterial strains, compared to the free drug.

**Table 6:** Antibacterial activity of unloaded and ciprofloxacin-loaded nanoparticles, compared to that of free ciprofloxacin against *Escherichia coli* K12.

Samples	Time of incubation [h]					
	5		24		48	
	CFU/ml $\times 10^{-5}$	Reduction of cells [%]	CFU/ ml $\times 10^{-5}$	Reduction of cells [%]	CFU/ml $\times 10^{-5}$	Reduction of cells [%]
E. coli K12 (untreated control)	3.2	-	3.2	-	7.8	-
PBCN (control) 2000 $\mu\text{g/ml}$	3.2	-	3.2	-	7.8	-
CfH-PBCN (40/2000) $\mu\text{g}/$ ml	0.59	81.5	0.26	99.1	0.15	98.0
CfH (40 $\mu\text{g/ml}$ )	0.29	90.9	0.12	99.6	0.05	99.3

## Acknowledgements

The authors thank Dr Stoyan Miloshev for his expert assistance with GPC.

## Funding

This work was supported by the Research and Development Fund of the University of Chemical Technology and Metallurgy, Bulgaria (grant 114,94).

## References

- Van Bambeke F, Michot JM, Van Eldere J, Tulkens PM (2005) Quinolones in 2005: an update. *Clin Microbiol Infect* 11: 256–280. [Link: https://goo.gl/PU35Yc](https://goo.gl/PU35Yc)
- Marchesan S, Qu Y, Waddington LJ, Easton CD, Glattauer V et al. (2013) Self-assembly of ciprofloxacin and a tripeptide into an antimicrobial nanostructured hydrogel. *Biomaterials* 34: 3678-3687. [Link: https://goo.gl/0VniH1](https://goo.gl/0VniH1)
- Rajagopalan-Levasseur P, Dournon E, Dameron G, Vilde JL, Pocard JJ (1990) Comparative Postantibacterial Activities of Pefloxacin, Ciprofloxacin, and Ofloxacin against Intracellular Multiplication of *Legionella pneumophila* Serogroup 1. *Antimicrob Agents Chemother* 34: 1733–1738. [Link: https://goo.gl/v3DI3n](https://goo.gl/v3DI3n)
- Letafat B, Emami S, Mohammadhosseini N, Faramarzi MA, Samadi N, et al. (2007) Synthesis and antibacterial activity of new N-[2-(thiophen-3-yl)ethyl] piperazinyl quinolones. *Chem Pharm Bull (Tokyo)* 55: 894–898. [Link: https://goo.gl/m5EUvH](https://goo.gl/m5EUvH)
- Marquez B, Pourcelle V, Vallet CM, Mingeot-Leclercq MP, Tulkens PM, et al. (2014) Pharmacological Characterization of 7-(4-(Piperazin-1-yl)) Ciprofloxacin Derivatives: Antibacterial Activity, Cellular Accumulation, Susceptibility to Efflux Transporters, and Intracellular Activity. *Pharm Res* 31: 1290–1301. [Link: https://goo.gl/r1uNHe](https://goo.gl/r1uNHe)
- Dillen K, Vandervoort J, Van den Mooter G, Verheyden L, Ludwig A (2004) Factorial design, physicochemical characterisation and activity of ciprofloxacin-PLGA nanoparticles. *Int J Pharm* 275: 171-187. [Link: https://goo.gl/dBjDdl](https://goo.gl/dBjDdl)
- Dillen K, Vandervoort J, Van den Mooter G, Ludwig A (2006) Evaluation of ciprofloxacin-loaded Eudragit® RS100 or RL100/PLGA nanoparticles. *Int J Pharm* 314: 72-82. [Link: https://goo.gl/60HpA3](https://goo.gl/60HpA3)
- Du J, El-Sherbiny IM, Smyth HD (2014) Swellable Ciprofloxacin-Loaded Nano-Micro Hydrogel Particles for Local Lung Drug Delivery. *AAPS Pharm Sci Tech* 15: 1535-1544. [Link: https://goo.gl/M2fZ7W](https://goo.gl/M2fZ7W)
- Jeong YI, Na HS, Seo DH, Kim DG, Lee HC, et al. (2008) Ciprofloxacin-encapsulated poly(dl-lactide-co-glycolide) nanoparticles and its antibacterial activity. *Int J Pharm* 352: 317-323. [Link: https://goo.gl/19LD71](https://goo.gl/19LD71)
- Kumar GV, Su CH, Velusamy P (2016) Ciprofloxacin loaded genipin cross-linked chitosan/heparin nanoparticles for drug delivery application. *Materials Letters* 180: 119-122. [Link: https://goo.gl/4mWTnD](https://goo.gl/4mWTnD)
- Kutscher M, Cheow WS, Werner V, Lorenz U, Ohlsen K, et al. (2015) Influence of salt type and ionic strength on self-assembly of dextran sulfate-ciprofloxacin nanoplexes. *Int J Pharm* 486: 21-29. [Link: https://goo.gl/EwSHkk](https://goo.gl/EwSHkk)
- Najafi SHM, Baghaie M, Ashori A (2016) Preparation and characterization of acetylated starch nanoparticles as drug carrier: Ciprofloxacin as a model. *Int J Biol Macromol* 87: 48–54. [Link: https://goo.gl/ukKXCh](https://goo.gl/ukKXCh)
- Silva-Jr AA, Scarpa MV, Pestana KC, Mercuri LP, de Matos JR, et al. (2008) Thermal analysis of biodegradable microparticles containing ciprofloxacin hydrochloride obtained by spray drying technique. *Thermochimica Acta* 467: 91–98. [Link: https://goo.gl/psl1kf](https://goo.gl/psl1kf)
- Baelo A, Levato R, Julian E, Crespo A, Astola J, et al. (2015) Disassembling bacterial extracellular matrix with DNase-coated nanoparticles to enhance antibiotic delivery in biofilm infections. *J Control Release* 209: 150–158. [Link: https://goo.gl/OxmZVq](https://goo.gl/OxmZVq)
- Fawaz F, Guyot M, Laguény AM, Devissaguet JPh (1997) Ciprofloxacin-loaded polyisobutylcyanoacrylate nanoparticles: preparation and characterization. *Int J Pharm* 154: 191-203. [Link: https://goo.gl/7akWfE](https://goo.gl/7akWfE)
- Fawaz F, Bonini F, Maugein J, Laguény AM (1998) Ciprofloxacin-loaded polyisobutylcyanoacrylate nanoparticles: pharmacokinetics and in vitro antimicrobial activity. *Int J Pharm* 168: 255-259. [Link: https://goo.gl/sgu3oN](https://goo.gl/sgu3oN)
- Page-Clisson ME, Pinto-Alphandray H, Ourevitch M, Andremont A, Couvreur P (1998) Development of ciprofloxacin-loaded nanoparticles: physicochemical study of the drug carrier. *J Control Release* 56: 23-32. [Link: https://goo.gl/osD6Ro](https://goo.gl/osD6Ro)
- Page-Clisson ME, Alphandary HP, Chachaty R, Couvreur P, Andremont A (1998) Drug targeting by polyalkylcyanoacrylate nanoparticles is not efficient against persistent *Salmonella*. *Pharm Res* 15: 544-549. [Link: https://goo.gl/7Qib1Y](https://goo.gl/7Qib1Y)
- Garcia LG, Lemaire S, Kahl BC, Becker K, Proctor RA, et al. (2013) Antibiotic activity against small-colony variants of *Staphylococcus aureus*: review of in vitro, animal and clinical data. *J Antimicrob Chemother* 68: 1455–1464. [Link: https://goo.gl/om1KZd](https://goo.gl/om1KZd)
- Rangelova N, Georgieva N, Mileva K, Yuryev R, Müller R (2012) Synthesis and antibacterial activity of SiO<sub>2</sub>-CMC-Ag hybrid materials prepared by sol-gel method. *Compt Rend Acad Bulg Sci* 65: 1057-1064. [Link: https://goo.gl/T4nw5x](https://goo.gl/T4nw5x)
- Behan N, Birkinshaw C, Clarke N (2001) Poly *n*-butyl cyanoacrylate nanoparticles: a mechanistic study of polymerisation and particle formation. *Biomaterials* 22: 1335–1344. [Link: https://goo.gl/aDxbkJ](https://goo.gl/aDxbkJ)
- Romaňuk CB, Garro LY, Chattah AK, Monti GA, Cuffini SL, et al. (2010) Crystallographic, thermal and spectroscopic characterization of a ciprofloxacin saccharinate polymorph. *Int J Pharm* 391: 197–202. [Link: https://goo.gl/ZA6R1r](https://goo.gl/ZA6R1r)
- Simeonova M, Velichkova R, Ivanova G, Enchev V, Abrahams I (2004) Study on the role of 5-fluorouracil on the polymerization of butylcyanoacrylate during the formation of nanoparticles. *J Drug Targeting* 12: 49-56. [Link: https://goo.gl/EW4xrx](https://goo.gl/EW4xrx)
- Beyer R, Pestova E, Millichap JJ, Stosor V, Noskin GA, et al. (2000) A convenient assay for estimating the possible involvement of efflux of fluoroquinolones by *Streptococcus pneumoniae* and *Staphylococcus aureus*: evidence for diminished moxifloxacin, sparfloxacin, and trovafloxacin efflux. *Antimicrob Agents Chemother* 44: 798–801. [Link: https://goo.gl/3B1xJS](https://goo.gl/3B1xJS)

25. Peterson LR (2001) Quinolone Molecular Structure-Activity Relationships: What We Have Learned about Improving Antimicrobial Activity. *Clin Infect Dis* 33 (Supplement 3): S180–S186. [Link: https://goo.gl/FeqwmF](https://goo.gl/FeqwmF)
26. Piddock LJV, Zhu M (1991) Mechanism of sparfloxacin against and mechanism of resistance in gram-negative and gram-positive bacteria. *Antimicrob Agents Chemother* 35: 2423–2427. [Link: https://goo.gl/v1dZOP](https://goo.gl/v1dZOP)
27. Takenouchi T, Tabata F, Iwata Y, Hanzawa H, Sugawara M, et al. (1996) Hydrophilicity of quinolones is not an exclusive factor for decreased activity in efflux-mediated resistant mutants of *Staphylococcus aureus*. *Antimicrob Agents Chemother* 40: 1835–1842. [Link: https://goo.gl/1BdQwN](https://goo.gl/1BdQwN)
28. Yoshida H, Bogaki M, Nakamura S, Ubukata K, Konno M (1990) Nucleotide sequence and characterization of the *Staphylococcus aureus* norA gene, which confers resistance to quinolones. *J Bacteriol* 172: 6942–6949. [Link: https://goo.gl/qwsK9s](https://goo.gl/qwsK9s)
29. Zeller V, Janoir C, Kitzis MD, Gutmann L, Moreau NJ (1997) Active efflux as a mechanism of resistance to ciprofloxacin in *Streptococcus pneumoniae*. *Antimicrob Agents Chemother* 41:1973–1978. [Link: https://goo.gl/QKTj8a](https://goo.gl/QKTj8a)
30. Renjis TT, Suryanarayanan V, Reddy PG, Baskaran S, Pradeep T (2004) Ciprofloxacin-Protected Gold Nanoparticles. *Langmuir* 20: 1909-1914. [Link: https://goo.gl/CfZna5](https://goo.gl/CfZna5)
31. Momot KI, Kuchel PW (2003) Pulsed field gradient nuclear magnetic resonance as a tool for studying drug delivery systems. *Concepts Magn Reson Part A* 19: 51-64. [Link: https://goo.gl/k65KbN](https://goo.gl/k65KbN)
32. Simeonova M, Rangel M, Ivanova G (2013) NMR study of the supramolecular structure of dual drug-loaded poly (butyl cyanoacrylate) nanoparticles. *Phys Chem Chem Phys* 15: 16657-16664. [Link: https://goo.gl/wRNtTB](https://goo.gl/wRNtTB)
33. Romañuk CB, Garro LY, Chattah AK, Monti GA, Manzo RH, et al. (2009) Characterization of the solubility and solid-state properties of saccharin salts of fluoroquinolones. *J Pharm Sci* 98: 3788-3801. [Link: https://goo.gl/beJqC7](https://goo.gl/beJqC7)

**Copyright:** © 2017 Simeonova MY, et al. This is an open-access article distributed under the terms of the Creative Commons Attribution License, which permits unrestricted use, distribution, and reproduction in any medium, provided the original author and source are credited.